

On the Partonometry of $V(= \gamma, W, Z)$ +jet Events at Hadron Colliders

V. A. Khoze^a and W. J. Stirling^{a,b}

^a *Department of Physics, University of Durham, Durham, DH1 3LE*

^b *Department of Mathematical Sciences, University of Durham, Durham, DH1 3LE*

Abstract

Significant colour interference effects are expected in $V(= \gamma, W, Z)$ +jet production at hadron colliders. These directly influence the hadronic antenna patterns and can provide a valuable diagnostic tool for probing the nature of the underlying parton subprocesses. Motivated by these ideas, we present quantitative predictions for the distributions of soft particles and jets in W +jet production at the Tevatron $p\bar{p}$ collider.

It was realised long ago [1–4] that the overall structure of particle angular distributions in multijet events in hard scattering processes (the event portrait) is governed by the underlying colour dynamics at short distances. A natural idea has been proposed [1–8] (for recent detailed studies see Ref. [9]) to use this colour event portrait as a “partonometer” mapping the basic interaction short-distance process. The interest in this subject has recently been boosted because of two reasons. First, as was advocated in Ref. [9], the hadronic antenna pattern can be used as a diagnostic tool to dissect the colour structure of the exciting large- E_T jet events observed by CDF [10] and D0 [11] at the Tevatron $p\bar{p}$ collider, as a way to distinguish between conventional QCD and possible new physics production mechanisms. Secondly, both CDF and D0 have started very successfully [12–15] to measure the structure of multijet events and have demonstrated that the distinctive colour interference effects survive the hadronization stage and are clearly visible in the data. It has been known for a long time [2] that an especially bright colour interference effect arises in the case of large- E_T production of colour singlet objects, for instance, in V +jet events (with $V = \gamma, W^\pm$ or Z). The hadronic antenna patterns for to such processes are entirely analogous to that in the celebrated string [16] or drag [17] effect in $e^+e^- \rightarrow q\bar{q}g$ events.

Recently the first (very impressive) data on W +jet production from D0 [14, 15] have become available. The colour coherence effects are clearly seen and in our view these studies have a very promising future. They may play the same role for hadron colliders as the important series of results on inter-jet studies at e^+e^- colliders.

The purpose of this paper is to present quantitative predictions for the colour interference phenomena in the distribution of soft particles and jets in V +jet production at hadron colliders, in particular the Tevatron $\sqrt{s} = 1.8$ TeV $p\bar{p}$ collider.

There are two leading-order processes, $q\bar{q} \rightarrow Vg$ and $qg \rightarrow Vq$. Each has its own distinctive antenna pattern, as we shall see. In principle, the antenna pattern could be used as a ‘partonometer’ to identify the dominant scattering process.

There are two experimental methods which are likely to prove useful. With sufficiently high statistics, one could use an additional soft jet as the probe of the antenna pattern. Alternatively, with fewer events one could use the distribution of soft hadrons without requiring jet reconstruction. Both of these quantities are directly related to the inclusive soft gluon distribution in the NLO processes $q\bar{q} \rightarrow Vgg$ and $qg \rightarrow Vqg$. We will consider such distributions, first in the soft-gluon approximation where the results are particularly simple, and then using the exact QCD matrix elements and phase space constraints.

The distribution of soft gluon radiation is controlled by the basic antenna pattern (see for example Ref. [3])

$$[ij] \equiv \frac{p_i \cdot p_j}{p_i \cdot k p_j \cdot k} = \frac{1 - \mathbf{n}_i \cdot \mathbf{n}_j}{E_k^2 (1 - \mathbf{n}_k \cdot \mathbf{n}_i) (1 - \mathbf{n}_k \cdot \mathbf{n}_j)}, \quad (1)$$

where the $p_i^\mu = E_i(1, \mathbf{n}_i)$ are the four-momenta of the partons participating in the hard scattering process. This corresponds to the emission of soft primary gluons with energies E_k : $\Lambda_{QCD} \ll E_k \ll E_i, E_j$. The particle flow is then described by extra multiplicative cascading factors, see below. Since the parton scattering process acts as a colour antenna, the distribution of soft particle flows between the jets is determined by the overall colour structure of the event [1–3,17]

In order to make the study more quantitative we must define appropriate kinematic distributions and then compute the contributions of the various subprocesses. In order to fully understand the differences between these, we first consider the soft gluon distribution at the parton-parton scattering level with fixed kinematics. The generic process is

$$a(p_1) + b(p_2) \rightarrow c(p_3) + d(p_4) + g(k) , \quad (2)$$

where the gluon is soft relative to the two large- E_T partons c and d . We assume massless quark and gluon partons and write M_V for the mass of the vector boson. In our quantitative studies, we are particularly interested in the angular distribution of the soft gluon around one of the large- E_T final-state particles, p_3 say. Using the notation $p^\mu = (E, p_x, p_y, p_z)$, we write

$$\begin{aligned} p_3^\mu &= (M_T \cosh \eta, 0, E_T, M_T \sinh \eta) , \\ k^\mu &= (k_T \cosh(\eta + \Delta\eta), k_T \sin \Delta\phi, k_T \cos \Delta\phi, k_T \sinh(\eta + \Delta\eta)) , \end{aligned} \quad (3)$$

where $M_T = E_T$ for $c = q, g$ and $M_T = \sqrt{E_T^2 + M_V^2}$ for $c = V$. The phase-space separation between the soft gluon and parton c is parametrized by $\Delta\eta$ and $\Delta\phi$. Alternative variables, more suited to the experimental analysis, are the radial and polar angle variables in the ‘‘LEGO plot’’:

$$\begin{aligned} \Delta\eta &= \Delta R \cos \beta , \\ \Delta\phi &= \Delta R \sin \beta . \end{aligned} \quad (4)$$

which are defined in such a way that the LEGO-plot separation between soft jet k and hard jet/vector boson p_3 is $R(k, p_3) = \sqrt{\Delta\eta^2 + \Delta\phi^2} = \Delta R$, ($0 \leq \Delta R < \infty$), and the azimuthal orientation of k around p_3 in the LEGO plot is parametrized by the angle β , ($0 \leq \beta < 2\pi$). Our convention is such that $\beta = 0$ corresponds to the direction of the incoming parton a , i.e. $p_{1z} > 0$.

In terms of these variables, the soft gluon phase space is

$$\frac{1}{(2\pi)^3} \frac{d^3k}{2E_k} = \frac{1}{16\pi^3} k_T dk_T \Delta R d\Delta R d\beta . \quad (5)$$

We will be particularly interested in the behaviour of the cross section as a function of β for fixed $k_T, \Delta R$ and fixed E_T, η .

The matrix elements for the lowest-order processes (for the case $V = W$) are:¹

$$\begin{aligned} \overline{\sum} |\mathcal{M}|^2(q(p_1)\bar{q}(p_2) \rightarrow W(p_3)g(p_4)) &= \frac{g_s^2 g_W^2}{4} \left(1 - \frac{1}{N_c^2}\right) \frac{t^2 + u^2 + 2sM_W^2}{tu} , \\ \overline{\sum} |\mathcal{M}|^2(q(p_1)g(p_2) \rightarrow W(p_3)q(p_4)) &= \frac{g_s^2 g_W^2}{4} \frac{1}{N_c} \frac{t^2 + s^2 + 2uM_W^2}{-ts} , \end{aligned} \quad (6)$$

¹CKM factors are omitted for clarity.

where $s = (p_1 + p_2)^2$, $t = (p_1 - p_3)^2$ and $u = (p_1 - p_4)^2$. In the soft-gluon approximation, the corresponding $2 \rightarrow 3$ matrix elements are [2]

$$\begin{aligned}\overline{\sum}|\mathcal{M}|^2(q\bar{q} \rightarrow Wg(g)) &= g_s^2 N_c \left([14] + [24] - \frac{1}{N_c^2} [12] \right) \overline{\sum}|\mathcal{M}|^2(q\bar{q} \rightarrow Wg) \\ \overline{\sum}|\mathcal{M}|^2(qg \rightarrow Wq(g)) &= g_s^2 N_c \left([12] + [24] - \frac{1}{N_c^2} [14] \right) \overline{\sum}|\mathcal{M}|^2(qg \rightarrow Wq)\end{aligned}\quad (7)$$

Note that for these processes, the effect of the soft gluon emission is simply to multiply the lowest-order matrix elements squared by an overall factor consisting of three different antennae, defined according to (1), one of which is suppressed in the large N_c limit. This structure is universal for any electroweak boson + jet production, i.e. $V = W^\pm, Z^0, \gamma, \gamma^*$. Although we shall only study the $V = W$ case in detail, similar results can be obtained for the other cases as well.²

To illustrate the colour coherence properties of the above scattering processes, we first show results for a very simple kinematic configuration, $2 \rightarrow 2$ scattering at 90° in the parton centre-of-mass frame, i.e. $\eta = 0$ in Eq. (3). For the case when the ‘target’ final-state particle (with momentum p_3) is a W boson, the matrix elements squared are as given above and the various antennae which contribute to the radiation pattern are, in terms of the variables ΔR and β ,

$$\begin{aligned}[12] &= 2, \\ [14] &= \frac{\exp(\Delta R \cos \beta)}{\cosh(\Delta R \cos \beta) + \cos(\Delta R \sin \beta)}, \\ [24] &= \frac{\exp(-\Delta R \cos \beta)}{\cosh(\Delta R \cos \beta) + \cos(\Delta R \sin \beta)}.\end{aligned}\quad (8)$$

where an overall factor of $1/k_T^2$ has been omitted from the right-hand sides. When the target final-state particle is the quark or gluon, i.e. for the subprocesses $q\bar{q} \rightarrow gW$ and $qg \rightarrow qW$, the corresponding results are obtained by interchanging the momenta p_3 and p_4 in Eq. (7).

Fig. 1 shows the angular (β) distribution of the soft gluon jet around each of the two large- E_T final-state particles, for $\Delta R = 1$. The quantity plotted is

$$\mathcal{R} = k_T^2 g_s^{-2} \frac{\overline{\sum}|\mathcal{M}_3|^2}{\overline{\sum}|\mathcal{M}_2|^2}, \quad (9)$$

where the $|\mathcal{M}_n|^2$ are the $2 \rightarrow n$ matrix elements squared of Eqs. (7) and (6). Also shown for reference in Fig. 1 is the radiation pattern for the process $q\bar{q} \rightarrow VV$, for which $\mathcal{R} = 4C_F = 16/3$, independent of β .

For the processes $q\bar{q} \rightarrow Wg$ and $q\bar{q} \rightarrow gW$, the distribution is symmetric about $\beta = 90^\circ$ and much larger for the latter, as expected. Notice that the soft gluon distribution around the W in $q\bar{q} \rightarrow Wg$ is smaller than that around the W in $q\bar{q} \rightarrow WW$; the away-side gluon

²In particular, the results for Z^0 +jet production will be almost identical to those for W +jet production, but in practice the event rates are an order of magnitude smaller.

jet in the former ‘drags’ the soft gluon away from the W hemisphere. In the formal limit $\Delta R \rightarrow 0$ we find, for this simple kinematic configuration,

$$\begin{aligned}\mathcal{R}(q\bar{q} \rightarrow Wg) &\rightarrow N_c \left(1 - \frac{2}{N_c^2}\right) = \frac{7}{3}, \\ \mathcal{R}(q\bar{q} \rightarrow gW) &\sim \frac{4N_c}{(\Delta R)^2}.\end{aligned}\tag{10}$$

The divergent behaviour in the latter case reflects the matrix-element singularity when the final-state soft and hard gluons are collinear.

The processes $qg \rightarrow Wq$ and $qg \rightarrow qW$ have asymmetric β distributions in Fig. 1. In both cases the distribution is larger in the *backward* ($\beta > 90^\circ$) hemisphere, i.e. when the soft gluon moves in the same direction as the incoming gluon. In fact the distribution for the $qg \rightarrow qW$ case is entirely analogous to that for $e^+e^- \rightarrow q\bar{q}g$, where the colour flow dynamics (string [16] or drag [17] effect) leads to a suppression of soft radiation between the outgoing quark and antiquark.

The corresponding $\Delta R \rightarrow 0$ limits are (cf. Eq. (10))

$$\begin{aligned}\mathcal{R}(qg \rightarrow Wq) &\rightarrow N_c \left(\frac{5}{2} - \frac{1}{2N_c^2}\right) = \frac{22}{3}, \\ \mathcal{R}(qg \rightarrow qW) &\sim \frac{4C_F}{(\Delta R)^2}.\end{aligned}\tag{11}$$

We next address the question of whether the differences between the $q\bar{q}$ and qg subprocesses shown in Fig. 1 survive a more rigorous calculational treatment. We do this in two stages: first we compare the simple analytic soft-gluon approximation to the $2 \rightarrow 3$ matrix elements with the exact result, and then we include the effects of phase space, realistic experimental cuts, parton distributions etc.

Fig. 2 compares the exact and approximate calculations of the distributions of Fig. 1. The exact $2 \rightarrow 3$ matrix elements squared are calculated using the spinor techniques of Ref. [19]. Exact $2 \rightarrow 3$ kinematics are used, i.e. having fixed p_3 and k we define $\vec{p}_4 = -\vec{p}_3 - \vec{k}$ and $E_4^2 = |\vec{p}_4|^2 + m_4^2$. Results are displayed using three different values of the soft gluon transverse momentum k_T . Because the ratio of matrix elements squared is multiplied by k_T^2 , the analytic soft-gluon approximation (solid lines) is approached as $k_T \rightarrow 0$. Evidently the soft-gluon approximation gives a very good representation of the exact result even at quite large values of k_T/E_T .

The next step is to implement a full cross section calculation, including realistic cuts on the final state particles. We are interested in a final state consisting of a W boson and two hadronic jets. The W and one jet are produced centrally with large E_T , and the second jet is soft and required to lie in an annulus in the (η, ϕ) plane around either the W or the large- E_T jet. The two jets are labelled according to the ordering of their transverse momenta, $E_T(J) > E_T(j)$. For illustration, we use the following set of cuts:

$$\begin{aligned}p_T(W), E_T(J) &> 100 \text{ GeV}, & |\eta(W)|, |\eta(J)| &< 0.5, \\ E_T(j) &> 10 \text{ GeV}, & 0.7 < R(J \text{ or } W, j) &< 1.3.\end{aligned}\tag{12}$$

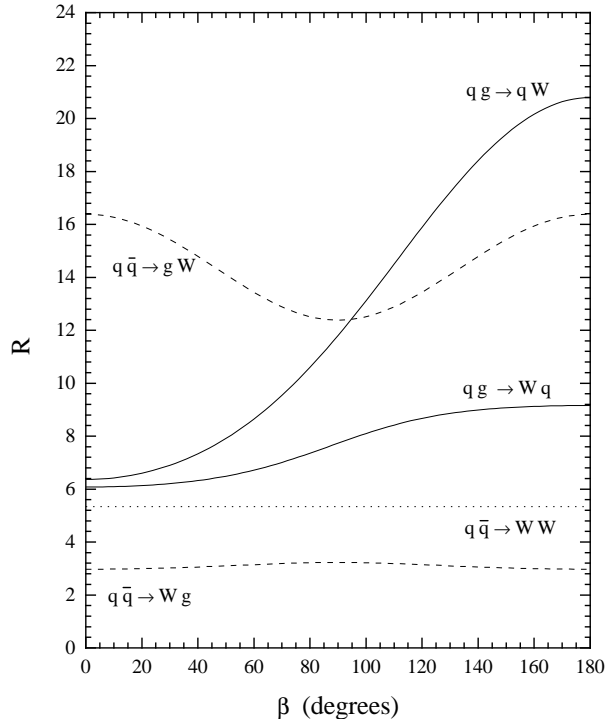


Figure 1: Ratio \mathcal{R} of the $2 \rightarrow 3$ and $2 \rightarrow 2$ matrix elements squared times k_T^2/g_s^2 as a function of the soft gluon azimuthal angle about the large- E_T jet or W , for the two subprocesses.

In addition, we use the MRS(R2) ($\alpha_s(M_Z^2) = 0.120$) parton distributions from Ref. [18]. One of the strong couplings is evaluated at scale $\mu = E_T(J)$ and the other at $\mu = E_T(j)$.

Fig. 3 shows the β distributions calculated using the above cuts. The separate histograms correspond to the different initial states ($q\bar{q}$ and qg), and to the target particle (jet or W) at the centre of the annulus. The curves are normalized to the corresponding $W + 1$ jet lowest-order cross sections for the corresponding initial state, with the cuts of (12) imposed. It is instructive to compare Figs. 3 and 2. The most noticeable difference is the suppression of the distributions at $\beta = 0^\circ, 180^\circ$ in the full calculation. This has a simple kinematic explanation. For fixed values of the rapidities and transverse momenta of the W and large- E_T jet, the subprocess energy $\sqrt{\hat{s}}$ is maximal when the soft jet rapidity is largest, i.e. at $\beta = 0^\circ, 180^\circ$. These large $\sqrt{\hat{s}}$ configurations receive an additional suppression from the parton distribution functions. More importantly, the *relative* size of the various distributions is similar to that specified by the soft-gluon antennae and shown in Fig. 1. This is illustrated in Fig. 4, which shows (solid lines) the ratio of the ‘jet’ to ‘ W ’ distributions in Fig. 3 for the $q\bar{q}$ and qg initial

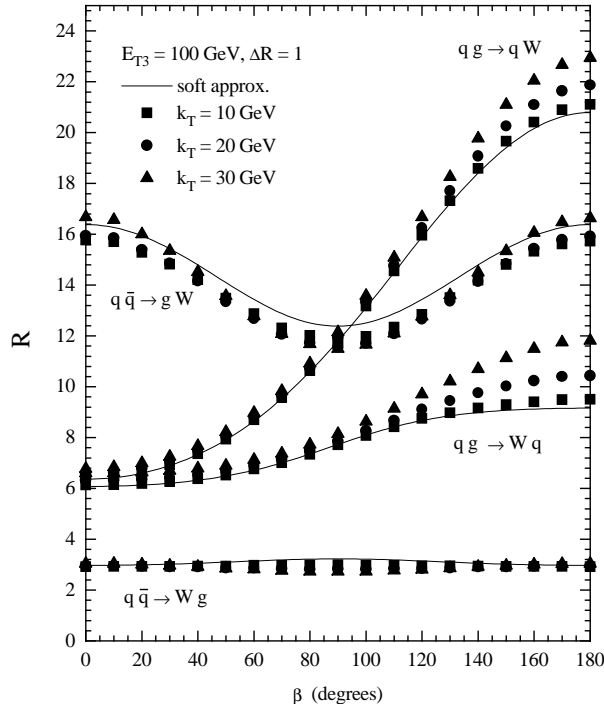


Figure 2: Ratio \mathcal{R} of the $2 \rightarrow 3$ and $2 \rightarrow 2$ matrix elements squared times k_T^2/g_s^2 as a function of the soft gluon azimuthal angle about the large- E_T jet or W , comparing the exact matrix element result (data points) for various values of the soft gluon k_T with the $k_T \rightarrow 0$ approximations of Fig. 1 (solid lines).

states.

For the qg processes, the agreement between the full calculation and the soft approximation is excellent.³ For the $q\bar{q}$ processes, the soft approximation appears to overestimate the result of the full calculation. However, this is due to the fact that the latter includes contributions from the ‘four-quark’ processes $q\bar{q} \rightarrow Wq\bar{q}$. Although these are formally sub-leading in the soft-jet limit ($k_T \rightarrow 0$), they make a non-negligible contribution for this choice of parameters and cuts. Including only the $q\bar{q} \rightarrow Wgg$ processes gives instead the dotted histogram, and agreement with the soft approximation is restored. Fig. 5 shows the β distribution when all subprocesses are included with their correct parton distribution weight-

³Note that in the full calculation ΔR is integrated over the range $0.7 < \Delta R < 1.3$ and the jet and W rapidities are integrated over the range $|\eta| < 0.5$, whereas in the soft approximation the antennae are calculated with $\Delta R = 1$ and $\eta = 0$.

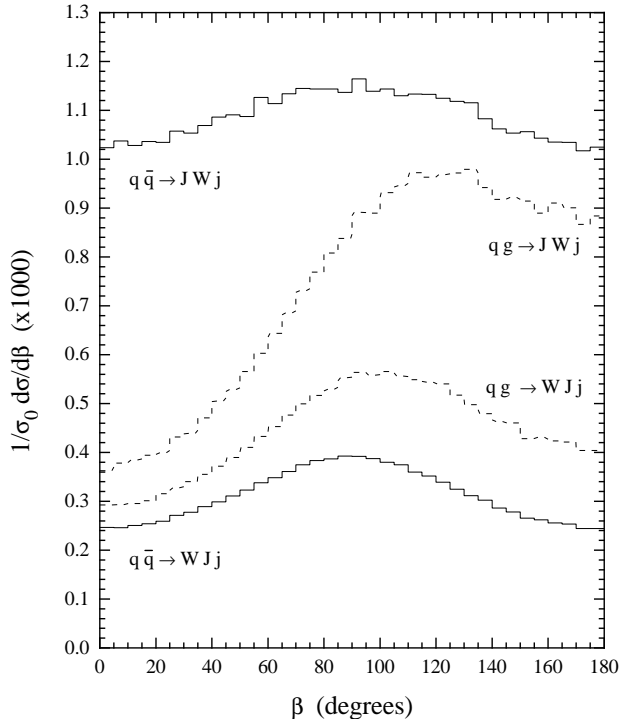


Figure 3: β distributions for the $W + 2$ jet cross sections at $\sqrt{s} = 1.8$ TeV, using exact $2 \rightarrow 3$ matrix elements with cuts as described in the text, for different initial states and target final state particles.

ing.⁴ For this choice of cuts, the $q\bar{q}$ and qg contributions are roughly equal, and so the net distribution interpolates between the separate distributions shown in Fig. 3. Note that in Fig. 5 the effect of including both qg and gq contributions is to symmetrize the distribution about $\beta = 90^\circ$. Fig. 6 shows the corresponding prediction for the ratio of the jet and W distributions, i.e. the analogue of Fig. 4 but including all parton subprocesses and cuts.

One problem with the analysis described above is that the event rate is very small. The requirement of a large E_T central jet and a large p_T central W strongly suppresses the cross section. Of course one solution would be to use a less restrictive set of cuts. Although this means that the asymptotic soft-gluon results are less applicable, the qualitative features of the colour dynamics are still apparent. As an example, Figs. 5 and 6 also show predictions

⁴The process $gg \rightarrow Wq\bar{q}$ is also included but makes a negligible contribution.

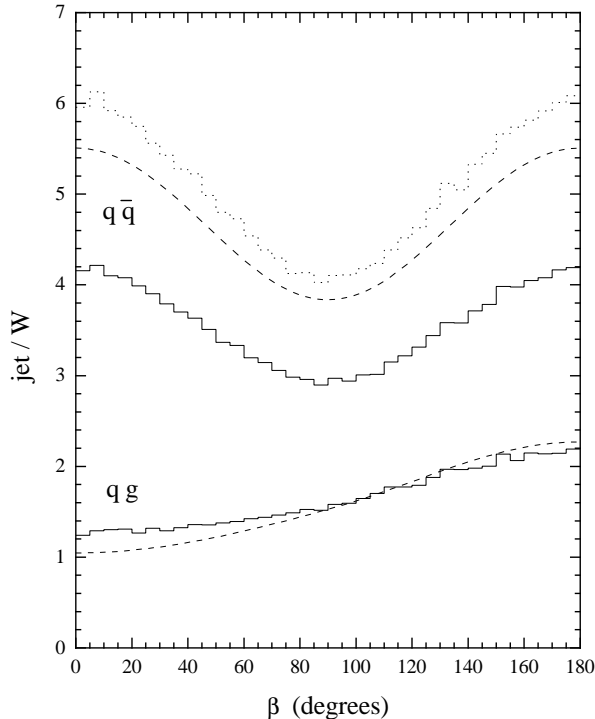


Figure 4: The ratios of jet/ W distributions from Fig. 3 for the $q\bar{q}$ and qg initial states. The dashed lines correspond to the soft-gluon approximation, and the solid histograms correspond to the exact calculation. In the dotted histogram, the $q\bar{q} \rightarrow Wq\bar{q}$ contribution is absent.

for a looser set of cuts:

$$\begin{aligned}
 p_T(W), E_T(J) > 30 \text{ GeV} , & \quad |\eta(W)|, |\eta(J)| < 1.0 , \\
 E_T(j) > 10 \text{ GeV} , & \quad 0.7 < R(J \text{ or } W, j) < 1.3 .
 \end{aligned}
 \tag{13}$$

The effect of loosening the cuts is to slightly increase the relative contribution of the $q\bar{q}$ subprocess, which has the effect of enhancing the jet/ W ratio. The following table lists the values of this ratio for jets produced in the transverse plane ($\beta = \pi/2$) and in the event plane ($\beta = 0, \pi$).

	$\beta = (0, \pi)$	$\beta = \pi/2$
tight cuts	2.7	2.1
loose cuts	3.2	2.4

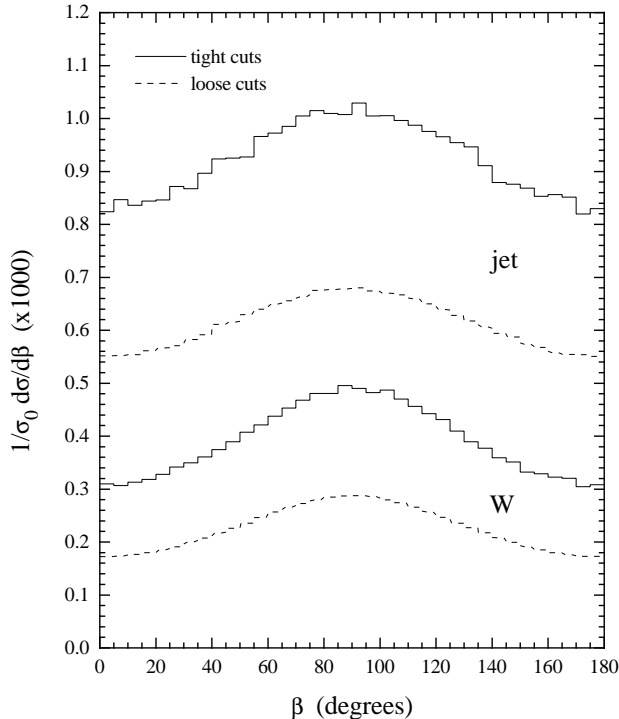


Figure 5: β distributions for the $W + 2$ jet cross sections at $\sqrt{s} = 1.8$ TeV, with cuts as described in the text and including all subprocesses.

A higher event rate could also be achieved by studying the distribution of soft jets in large E_T γ +jet production, which should exhibit the same qualitative features as W +jet production, although there may be experimental problems in obtaining a truly isolated large E_T photon sample. In fact, an additional theoretical advantage of γ +jet production is that there is a stronger dependence on E_T of the subprocess decomposition, i.e. the relative amounts of $q\bar{q}$ and qg scattering. This arises because the average momentum fraction of the initial-state partons is $\langle x \rangle \sim 2E_T/\sqrt{s}$, in contrast to $\langle x \rangle \sim (\sqrt{M_W^2 + E_T^2} + E_T)/\sqrt{s}$ for W +jet production. Note that this argumentation only applies to *central* V +jet production. In principle one can also study large E_T events where both the V and the jet have large and comparable rapidities, such that one of the momentum fractions becomes large and the other small. The effect of this is to enrich the contribution from qg scattering, thus modifying the β distribution according to Fig. 4.

An alternative approach, which requires much less luminosity, is to study the structure of *particle* (rather than *jet*) flows in the hard scattering events, see Refs. [1–3,17]. Here, unlike

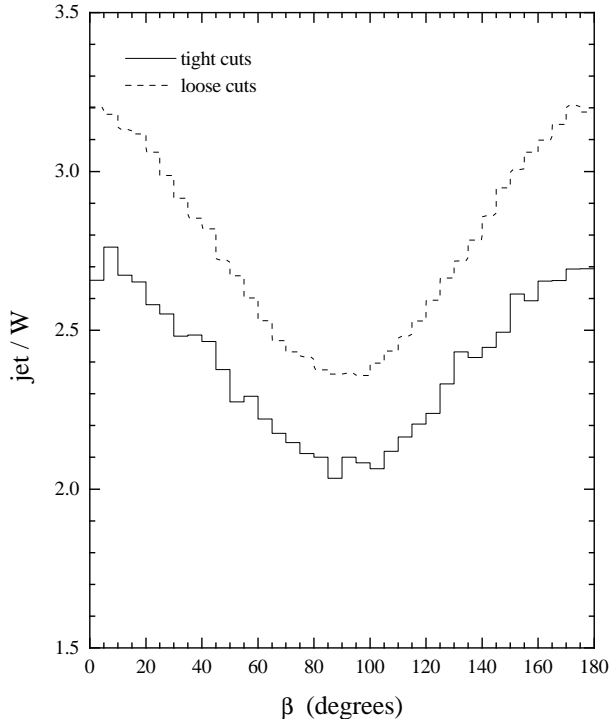


Figure 6: The ratios of jet/ W distributions from Fig. 5 for the two sets of cuts described in the text.

in the case of jet production, the geometry of the primary parton system is practically undisturbed, and there is of course no dependence on the jet-finding algorithm. Using soft particles, the colour coherence phenomena can be studied even when the overall statistics are limited. However, there is a price to pay. The success of the application of the analytical perturbative description to the particle flow distributions is based on the hypothesis of Local Parton Hadron Duality (LPHD) (see Ref. [20]), which assumes that the production of hadrons is governed by the QCD radiophysics of colour flows. The LPHD hypothesis is very well confirmed by all existing data, thus demonstrating that colour coherence effects successfully survive the hadronization stage, see Ref. [21]. Care must also be taken when using soft particles to study the colour coherence properties of the hard scattering to avoid a significant background contamination from soft particles produced in the ‘underlying event’. In practice, this could necessitate a minimum p_T cut on the registered hadrons.

Within the LPHD approach the radiation pattern for wide-angle soft hadron (h) produc-

tion can be written in the parton-parton centre-of-mass system as (see Refs. [1, 17])

$$\frac{dn_h}{d\Omega_{\mathbf{n}}} = \frac{E_k^2}{8\pi N_c g_s^2} \frac{\overline{\sum} |\mathcal{M}_3|^2}{\overline{\sum} |\mathcal{M}_2|^2} \left[N_g^h(E_T) \right]' , \quad (14)$$

where

$$\left[N_g^h(E_T) \right]' \equiv \frac{dN_g^h(E_T)}{d \ln E_T} \quad (15)$$

and $N_g^h(E_T)$ is the multiplicity of hadrons h in an individual gluon jet with hardness E_T . For the case when there is an experimental lower limit on the transverse energy of the registered hadron,

$$E_T \gg E_T^{\min} \gg \Lambda_{QCD} , \quad (16)$$

then the last factor in Eq. (14) becomes

$$\left[N_g^h(E_T) \right]' \longrightarrow \left[N_g^h(E_T) \right]' - \left[N_g^h(E_T^{\min}) \right]' . \quad (17)$$

The cascading factor $\left[N_g^h(E_T) \right]'$ takes into account the fact that the registered hadron h is a part of the cascade initiated by a soft gluon jet g . It originates in the evolution equation for jet multiplicity to order $\sqrt{\alpha_s}$ (for details see Refs. [2, 3, 17]):

$$N'_g(E) = \int^E \frac{dE_g}{E_g} 4N_c \frac{\alpha_s(E_g)}{2\pi} N_g(E_g) . \quad (18)$$

Note that asymptotically

$$N'_g(E) = \frac{C_F}{N_c} N'_g(E) \quad (19)$$

with

$$\frac{N'_g(E)}{N_g(E)} = \sqrt{\frac{4N_c \alpha_s(E)}{2\pi}} \left[1 + O\left(\sqrt{\frac{\alpha_s}{\pi}}\right) \right] . \quad (20)$$

For instance, the exact result for charged particle production is (for details see Refs. [20, 22])

$$N_g^{\text{ch}}(E) = K^{\text{ch}} \Gamma(B) \left(\frac{z}{2}\right)^{-B+1} I_{B+1}(z) , \quad (21)$$

with

$$\begin{aligned} z &= \sqrt{\frac{16N_c}{b}} Y , \quad Y = \ln \frac{E}{Q_0} , \\ B &= \frac{1}{b} \left(\frac{11}{3} N_c + \frac{2n_f}{3N_c^2} \right) \\ b &= \frac{11N_c - 2n_f}{3} . \end{aligned} \quad (22)$$

Here I_ν is the Modified Bessel function. The values of the parameters K^{ch} and Q_0 are obtained from fits to the e^+e^- data [23, 21]:

$$K^{\text{ch}} \simeq 1.3 , \quad Q_0 \simeq 250 \text{ MeV} . \quad (23)$$

Finally, the distributions of charged particle flow accompanying the hard scattering processes $q\bar{q} \rightarrow Wg$ and $qg \rightarrow Wq$ are given by

$$\begin{aligned} \left. \frac{8\pi dn_h}{d\Omega_{\mathbf{n}}} \right|_{q\bar{q} \rightarrow Wg} &= \left([\widehat{14}] + [\widehat{24}] - \frac{1}{N_c^2} [\widehat{12}] \right) \frac{dN_g^{\text{ch}}}{dY}, \\ \left. \frac{8\pi dn_h}{d\Omega_{\mathbf{n}}} \right|_{qg \rightarrow Wq} &= \left([\widehat{12}] + [\widehat{24}] - \frac{1}{N_c^2} [\widehat{14}] \right) \frac{dN_g^{\text{ch}}}{dY}, \end{aligned} \quad (24)$$

where

$$[\widehat{ij}] = \frac{1 - \mathbf{n}_i \cdot \mathbf{n}_j}{(1 - \mathbf{n} \cdot \mathbf{n}_i)(1 - \mathbf{n} \cdot \mathbf{n}_j)}. \quad (25)$$

Note that these particle distributions take the form of an overall energy-dependent factor multiplying the *same* angular distributions as in the soft-gluon antenna patterns, Eq. (7) and Fig. 1. In studying the relative amounts of hadronic radiation near, say, the hard jet and the W , the dN_g^{ch}/dY factors cancel and the relative angular distribution can be obtained from the curves in Fig. 1, weighted according to the relative contributions of the $q\bar{q} \rightarrow Wg$ and $qg \rightarrow Wq$ subprocesses to the total W +jet cross section. Fig. 7 shows the jet/ W β -distribution ratio (i.e. the analogue of Fig. 6) for soft particle production. We assume here that the particles have much smaller transverse momenta than the hard jet and W , so that (i) there is essentially no phase-space suppression of the distributions, and (ii) the $q\bar{q} \rightarrow Wq\bar{q}$ process makes a negligible contribution. In addition, the distribution is integrated over the annuli⁵ $0.7 < \Delta R < 1.3$ around the jet and the W , which are produced centrally, $|\eta| < 0.5$. The curves correspond to different values of the hard jet E_T . In fact for E_T values in the range $20 \text{ GeV} \lesssim E_T \lesssim 100 \text{ GeV}$ the $q\bar{q}$ and qg subprocesses give approximately equal contributions. The dashed lines in Fig. 7 are the limiting ‘pure’ $q\bar{q}$ and qg ratios. Notice that the particle jet/ W ratios are very similar in magnitude to the soft-jet ratios shown in Fig. 6. i.e. when expressed in terms of this ratio, the colour coherence effects appear to be universal. However, there is an important caveat to this conclusion. In this study we are only calculating the *perturbative* contribution to the particle and jet flow, i.e. the contribution associated with gluon emission from the single hard scatter which produces the W and the jet. In practice, there will also be a (non-perturbative) contribution from the ‘underlying event’. The lower the particle/jet k_T threshold, the more important this contribution is likely to be. We would further expect this background contribution to be approximately uniform in the (η, ϕ) plane, thereby increasing the β distributions by a constant amount. This would have the effect of *decreasing* the jet/ W ratios shown in Figs. 6 and 7. Since we are assuming that in practice the transverse momentum threshold for particle production will be much lower than for soft jet production, we would expect to see a larger effect in the former jet/ W ratio.

In conclusion, the aim of this paper has been to exemplify the application of the radio-physics of colour flows to the partonometry of $V(= \gamma, W, Z)$ +jet events in hadron-hadron collisions. As was appreciated long ago [1, 2], the colour interference effects accompanying such processes can be especially spectacular. They may well play for hadron colliders the

⁵Recall that the curves in Fig. 1 are evaluated at $\Delta R = 1$.

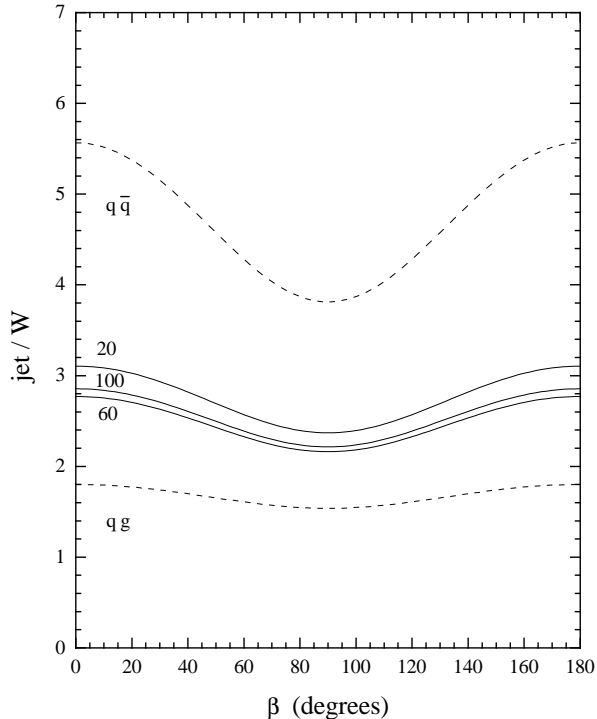


Figure 7: The ratios of jet/ W particle distributions, for different values of the jet $E_T = 20, 60, 100$ GeV. The dashed lines are the ‘pure’ $q\bar{q}$ and qg ratios.

same role as the celebrated string [16] and drag [17] phenomena observed in three jet production in e^+e^- annihilation. Clear experimental observation of the effects discussed in this paper, and the quantitative agreement with the basic formulae presented here, would lend strong support to the idea that hadronic antenna patterns can provide a valuable diagnostic tool for elucidating the underlying dynamics in multi-jet high E_T events. The first experimental results on W +jet production from the D0 collaboration [14, 15] look very promising.

Acknowledgements

We thank J. Ellis, A. Goshaw and N. Varelas for useful comments and discussions. This work was supported in part by the UK PPARC and the EU Programme “Human Capital and Mobility”, Network “Physics at High Energy Colliders”, contract CHRX-CT93-0357 (DG 12 COMA).

References

- [1] Yu.L. Dokshitzer, V.A. Khoze and S.I. Troyan, in Proc. 6th Int. Conf. on Physics in Collision, ed. M. Derrick (World Scientific, Singapore, 1987), p.417.
Yu.L. Dokshitzer, V.A. Khoze and S.I. Troyan, Sov. J. Nucl. Phys. **46** (1987) 712.
- [2] Yu.L. Dokshitzer, V.A. Khoze, A.H. Mueller and S.I. Troyan, Rev. Mod. Phys. **60** (1988) 373.
Yu.L. Dokshitzer, V.A. Khoze and S.I. Troyan in: Advanced Series on Directions in High Energy Physics, Perturbative Quantum Chromodynamics, ed. A.H. Mueller (World Scientific, Singapore), v. 5 (1989) 241.
- [3] Yu.L. Dokshitzer, V.A. Khoze, A.H. Mueller and S.I. Troyan, “Basics of Perturbative QCD”, ed. J. Tran Thanh Van, Editions Frontières, Gif-sur-Yvette, 1991.
- [4] R.K. Ellis, G. Marchesini and B.R. Webber, Nucl. Phys. **B286** (1987) 643; Erratum Nucl. Phys. **B294** (1987) 1180.
R.K. Ellis, presented at “Les Rencontres de Physique de la Vallée d’Aoste”, La Thuile, Italy, March 1987, preprint FERMILAB-Conf-87/108-T (1987).
- [5] Yu.L. Dokshitzer, V.A. Khoze and S.I. Troyan, Sov. J. Nucl. Phys. **50** (1989) 505.
- [6] Yu.L. Dokshitzer, V.A. Khoze and T. Sjöstrand, Phys. Lett. **B274** (1992) 116.
- [7] G. Marchesini and B.R. Webber, Nucl. Phys. **B330** (1990) 261.
- [8] D. Zeppenfeld, Madison preprint MADPH-95-933 (1996).
- [9] J. Ellis, V.A. Khoze and W.J. Stirling, CERN preprint CERN-TH/96-225 (1996), to be published in Zeit. Phys.
- [10] CDF Collaboration: F. Abe et al., Phys. Rev. Lett. **77** (1996) 438.
- [11] DØ Collaboration: G.C. Blazey, presented at the XXXI Rencontres de Moriond, QCD and High Energy Hadronic Interactions, Les Arcs, France, March 1996, Fermilab-Conf-96-132-E (1996).
- [12] CDF Collaboration: F. Abe et al., Phys. Rev. **D50** (1994) 5562. DØ Collaboration: S. Abachi et al., FERMILAB preprint, FERMILAB Conf-95/182-E.
N. Varelas, preprint FERMILAB, Conf-95/181-E, DØ and CDF; presented at the XXXI Rencontres de Moriond, Les Arcs, Savoie, France, March 23-30, 1996.
- [13] CDF Collaboration: A. Korytov presented at the *QCD’96* conference, Montpellier, France, July 1996, to appear in the Proceedings, Nucl. Phys. B (Proc. Suppl.), ed. S. Narison.
- [14] DØ Collaboration: D.E. Cullen-Vidal, presented at the Annual Divisional Meeting (*DPF96*) of the APS Division of Particles and Fields, Minneapolis, August 1996, FERMILAB preprint, FERMILAB Conf-96-304-EI (1996).

- [15] D0 Collaboration: H. Melanson, presented at INFN Eloisatron project 33rd Workshop, Erice, Italy,
- [16] B. Andersson, G. Gustafson and T. Sjöstrand, Phys. Lett. **B94** (1980) 211.
- [17] Ya.I. Azimov, Yu.L. Dokshitzer, V.A. Khoze and S.I. Troyan, Phys. Lett. **B165** (1985) 147; Sov. J. Nucl. Phys. **43** (1986) 95.
- [18] A.D. Martin, R.G. Roberts and W.J. Stirling, Phys. Lett. **B387** (1996) 419.
- [19] R. Kleiss and W.J. Stirling, Nucl. Phys. **B262** (1985) 235.
- [20] Ya.I. Azimov, Yu.L. Dokshitzer, V.A. Khoze and S.I. Troyan, Z. Phys. **C27** (1985) 65; **C31** (1986) 213.
- [21] For a recent review see: V.A. Khoze and W. Ochs, *Perturbative QCD Approach to Multiparticle Production*, University of Durham preprint DTP/96/36 (1996).
- [22] Yu.L. Dokshitzer, V.A. Khoze and S.I. Troyan, Int. J. Mod. Phys. **A7** (1992) 1875.
- [23] Yu.L. Dokshitzer, V.A. Khoze and S.I. Troyan, Z. Phys. **C55** (1992) 107.